Electrochimica Acta 58 (2011) 52–57

Contents lists available at SciVerse ScienceDirect

Electrochimica Acta

journal homepage: www.elsevier.com/locate/electacta

Preparation of PAA-g-CTAB/PANI polymer based gel-electrolyte and the application in quasi-solid-state dye-sensitized solar cells

Ziying Tang, Qin Liu, Qunwei Tang, Jihuai Wu*, Jiangli Wang, Shuhong Chen, Cunxi Cheng, Haijun Yu, Zhang Lan, Jianming Lin, Miaoliang Huang

Engineering Research Center of Environment-Friendly Functional Materials, Ministry of Education, Institute of Materials Physical Chemistry, Huaqiao University, Quanzhou 362021, China

ARTICLE INFO

Article history:
Received 24 June 2011
Received in revised form 21 August 2011
Accepted 21 August 2011
Available online 19 September 2011

Keywords:
Poly (acrylic acid)
CTAB, Polyaniline
Gel-electrolyte
Dye-sensitized solar cells

ABSTRACT

A microporous hybrid polymer of poly(acrylic acid)-g-cetyltrimethylammonium bromide/polyaniline (PAA-g-CTAB/PANI) was synthesized by a two-steps solution polymerization. Using this amphipathic hybrid as host, a gel-electrolyte with a high absorbency of 17.69 (g/g) and a high conductivity of 14.29 mS cm^{-1} was prepared. The polymer hosts have been characterized by means of scanning electron microscopy (SEM), and the microporous network structure was observed. Fourier transform infrared spectroscopy (FTIR) and the electrochemical property tests of the gel-electrolytes have been carried out by means of *I–V* measurements. The quasi-solid-state dye-sensitized solar cells (QS-DSSCs) based on the hybrid gel-electrolyte reach a light-to-current efficiency of 6.68%.

1. Introduction

Since the first prototype of a dye-sensitized solar cell (DSSC) was reported in 1991 by O'Regan and Gratzel [1], it has aroused an intensive interest over the past decades due to its low cost and simple preparation procedure [1,2]. Based on liquid electrolytes, a high photoelectric conversion efficiency over 11.4% for DSSC has been achieved [3,4]. However, the potential problems caused by the liquid electrolytes, such as the leakage and volatilization of liquid, are considered as some of the critical factors limiting the long-term performance and practical use of the DSSCs [5,6]. It has been pointed by Gratzel [3] that long-term stability is a key requirement for all types of solar cells, and a vast amount of tests have therefore been carried out over the last 15 years to scrutinize the stability of the DSSCs. Recently, many efforts have been done to replace liquid electrolyte with all-solid-state electrolyte [7–10], ionic liquid electrolyte [11–13] and quasi-solid-state gel-electrolyte [5,6,14–18]. Especially, the quasi-solid-state gel-electrolyte attracts a great attention due to its higher conductivity and excellent long-term stability. For all solid-state electrolyte, though which posses the best long-term stability, it still remains an important problem such as low conversion efficiency compared to the liquid electrolyte because of the low conductivity of the solid-state electrolyte itself, imperfect wetting of the porous TiO_2 film and the high recombination rate at the TiO_2/solid-state electrolyte interface [5,17]. In contrast, quasi-solid-state gel-electrolyte exhibits an ionic conductivity as high as that of liquid electrolyte, prevents the solvent from leaking and volatilizing, and which can be nicely cast onto porous TiO_2 [17]. The enhanced conversion efficiency and improved stability of quasi-solid-state gel-electrolyte dye-sensitized solar cells (QS-DSSCs) should accelerate the practical usage of DSSC. What's more, large area quasi-solid-state DSSC also have been fabricated in the previous works by Biancardo et al. [16] and satisfactory results were reached. The usage of quasi-solid-state electrolyte in large area DSSCs shows a promising prospect to fabricate high efficient and stabile DSSCs.

The gel-electrolyte consisted of a polymer host, a solvent and an ionic conductor. In most polymer gel electrolytes, the polymer content is low, usually less than 20%, and a significant amount of organic solvent is retained. The limitation of solvent leakage and volatilization is an important issue for preparing gel-electrolyte. As we know, poly(acrylic acid) (PAA) is a superabsorbent polymer with three-dimensional (3D) network and hydrophilic groups, it can absorb large amounts of liquid and the absorbed liquid is hardly to be released even under some pressure [19–21]. However, pure PAA is not a good absorbent for conventional organic solvent used in liquid electrolytes [6], due to the hydrophilic functional group of carboxyl groups in PAA. In order to improve their absorbency of organic solvents, a modification of the carboxyl groups or an introduction of amphiphilic groups is necessary.

* Corresponding author. Tel.: +86 595 22692229; fax: +86 595 22692229.
E-mail address: jhwu@hqu.edu.cn (J. Wu).

0013-4686/$ – see front matter © 2011 Elsevier Ltd. All rights reserved.
doi:10.1016/j.electacta.2011.08.074

In our previous work, by modifying PAA with amphiphilic poly(ethylene glycol) (PEG) [6], gelatin [20], glycerin [21], etc., we have successfully synthesized series of gel-electrolytes based on modified hybrid superabsorbents and which showed excellent stability and absorbent ability for liquid electrolyte [6]. In continuation of our studies, a microporous superabsorbent of poly(acrylic acid)-g-cetyltrimethylammonium bromide (PAA-g-CTAB) was prepared at the first stage, and followingly, aniline solution mixed with HCl was absorbed into and polymerized inside of the polymer network, and the PAA-g-CTAB/PANI hybrid polymer was obtained. Using the PAA-g-CTAB/PANI hybrid polymer as host, a gel-electrolyte with a high absorbency of 17.69 (g/g) and a high conductivity of 14.29 mS cm^{-1} was prepared. The gel-electrolyte is used to assemble QS-DSSCs, and a relatively high efficiency of 6.68% was achieved.

2. Experimental

2.1. Materials

Acrylic acid monomer, purchased from Shanghai Chemical Agent Company, China, was distilled under reduced pressure prior to use. Cetyltrimethylammonium Bromide (CTAB), purchased from Shanghai Chemical Agent Company. The organometallic Sensitized dye N-719 [$RuL_2(NCS)_2$, L = 4,4′-dicarboxylate-2,2′-bipyridine] was obtained from Solaronix SA (Switzerland). Titanium(IV) isopropoxide, PEG (formula weight of 20 000), OP emulsification agent (Triton X-100) and other reagents were obtained from Shanghai Chemical Agent, P.R. China and used as received. All other chemicals were analytical pure grade and were purchased from Xilong Chemicals. Crosslink agent N,N′-(dimethyl)acrylamide was purified by recrystallization from 66 vol% ethanol/water solution before using; other chemicals and solvents were used without further purification before using.

2.2. Synthesis of PAA-g-CTAB superabsorbent polymer

PAA-g-CTAB superabsorbent polymer was synthesized by modifying the procedure from Refs. [6,22–24]. 1.0 g CTAB and 10 g acrylic acid (AA) were dispersed in 15 ml distilled water. Subsequently, initiator potassium peroxydisulfate (KPS) (weight ratio of KPS to AA was 0.8%) and N,N′-methylene bisacrylamide (NMBA) (weight ratio of NMBA to AA was 0.05%) were added to the mixed solution system. Under a nitrogen atmosphere, a polymerization reaction took place under vigorous stirring at 80 °C. After the solution became viscous, the system was cooled to room temperature. After the solution became viscous, the system was cooled to room temperature, the resultant product was filtered through Whatman filter paper No. 54 and then washed in excess distilled water to remove any impurities. Finally, the product was vacuum dried at 80 °C for more than 12 h to a constant weight.

2.3. Preparation of PAA-g-CTAB/PANI hybrid superabsorbent and gel-electrolyte

PAA-g-CTAB/PANI hybrid was prepared according to the following procedures [22,23]: 0.2 g of PAA-g-CTAB was immersed in a predetermined amount of aniline (ANI) and HCl solution (1 ml ANI, 300 ml H_2O, pH = 2.5) at ambient temperature for more than 48 h, which resulted in the absorption of ANI monomer into the PAA-g-CTAB network and leaded to the formation of a swollen sample. The swollen sample was dispersed in a KPS solution of 15 ml containing 0.0365 M KPS (act as initiator and doping agent), which caused an in situ polymerization between ANI monomers and the formation of PANI inside the network of PAA-g-CTAB. The polymerization reaction took place at 4 °C for more than 48 h in dark. When the swollen sample changed from the original pale yellow color to dark green color, the PANI was formed inside of polymer network. After the polymerization, similar to the preparation of PAA-g-CTAB, the intermediate product was filtrated, washed, dried, thus a PAA-g-CTAB/PANI hybrid superabsorbent was obtained.

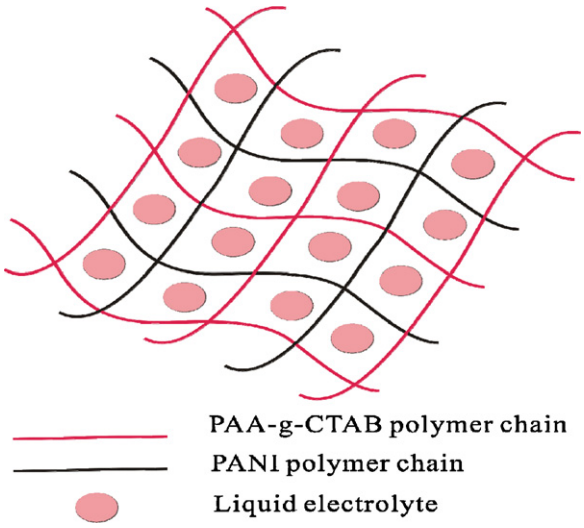

Scheme 1. Structure of PAA-g-CTAB/PANI hybrid superabsorbent.

The gel-electrolyte was prepared by soaking 0.2 g dried polymer sample in liquid electrolyte for more than 96 h to reach absorption saturation. The liquid electrolyte consisted of 0.1 M tetrabutylammonium iodide (TBAI), 0.1 M tetramethylammonium iodide (TMAI), 0.1 M tetraethylammonium iodide (TEAI), 0.1 M KI, 0.1 M LiI, 0.1 M NaI, 0.06 M I_2 in mixed organic solvent of N-methyl-2-pyrrolidone (NMP) and acetonitrile (AC) (NMP/AC = 2/8). Scheme 1 shows the structure of PAA-g-CTAB/PANI polymer based gel-electrolyte.

2.4. The assembling of DSSCs

A 10-μm-thick film of TiO_2 nanocrystal anode films was prepared by using a "doctor blade method". A QS-DSSC with PAA-g-CTAB or PAA-g-CTAB/PANI based gel-electrolyte was fabricated by sandwiching a slice of gel-electrolytes between dye-sensitized TiO_2 anode electrode and a platinum counter electrode. The detailed fabrication procedure for the nanocrystalline TiO_2 photoanodes and the assembly of DSSCs has been described by us elsewhere [6,25,26].

2.5. Characterizations

The morphology of PAA-g-CTAB and PAA-g-CTAB/PANI samples were studied by using a scanning electron microscope (SEM, Hitachi S-5200, Japan). The PAA-g-CTAB or PAA-g-CTAB/PANI sample was freeze dried by a freeze dryer (FD-1A-50, Beijing Boyikang Laboratory Instruments Co., Ltd, Beijing, China) and then cut into a slice and coated with gold, followingly its surface was observed and photographed by SEM. The groups of PAA-g-CTAB or other powdered samples were identified by Fourier transform infrared (FTIR) spectroscopy on a Nicolet Impact 410 FTIR spectrophotometer (Inspiratech 2000 Ltd, Warwickshire, UK) using KBr pellets.

2.6. Measurement

The swelling ratio (SR, g/g) of sample was measured according to the equation below [27]:

$$\text{Swelling ratio (SR)} = \frac{W_2 - W_1}{W_1} \quad (1)$$

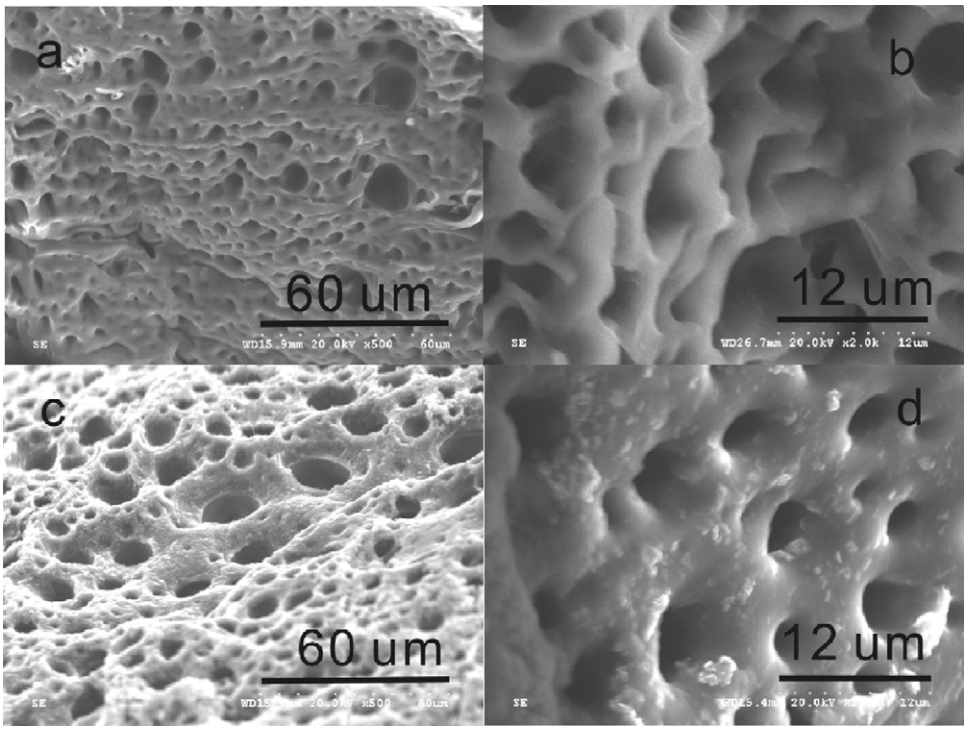

Fig. 1. SEMs of PAA-g-CTAB (a, b) and PAA-g-CTAB/PANI (c, d) polymers (at different magnifications).

where W_1 is the mass of dried sample (g), W_2 is the mass of swollen gel-electrolyte (g). The ionic conductivity of gel-electrolyte was measured by using model DDSJ-308 digitized conductivity meter (Shanghai Reici Instrument Factory, China). The instrument was calibrated with 0.01 M KCl aqueous solution prior to experiments [6].

2.7. Photovoltaic test

The photovoltaic test of DSSC was carried out by measuring the *J–V* characteristic curves under simulated AM 1.5 solar illumination at 100 mW cm^{-2} from a 100 W xenon arc lamp (XQ-500 W, Shanghai Photoelectricity Device Company, China) in ambient atmosphere. The fill factor (FF) and overall energy conversion efficiency (η) of the cell were calculated according to the following equations [6]:

$$\mathrm{FF} = \frac{V_{\max} \times J_{\max}}{V_{\mathrm{oc}} \times J_{\mathrm{sc}}} \quad (2)$$

$$\eta(\%) = \frac{V_{\max} \times J_{\max}}{P_{\mathrm{in}}} \times 100 = \frac{V_{\mathrm{oc}} \times J_{\mathrm{sc}} \times \mathrm{FF}}{P_{\mathrm{in}}} \times 100 \quad (3)$$

where J_{sc} is the short-circuit current density (mA cm^{-2}), V_{oc} is the open-circuit voltage (V), P_{in} is the incident light power, and $J_{\max}$ (mA cm^{-2}) and $V_{\max}$ (V) are the current density and voltage in the *J–V* curves at the point of maximum power output, respectively.

3. Results and discussions

3.1. The morphology of PAA-g-CTAB and PAA-g-CTAB/PANI polymers

The SEM images of PAA-g-CTAB and PAA-g-CTAB/PANI polymers were measured and shown in Fig. 1. From Fig. 1(a) and (b), it can be seen that the PAA-g-CTAB shows a microporous network structure, owing to this structure and hydrophilic group on it, a large amount of organic solvent can be absorbed, and the absorbed organic solvent is hardly removed under some pressure or heat, which is just the unique property of superabsorbent polymer [19,28]. When the ANI monomers are absorbed into the PAA-g-CTAB network and in situ polymerize in the network during the second polymerization process, PANI chains are formed inside of the PAA-g-CTAB network. Thus, an interpenetrating network structure of PAA-g-CTAB/PANI can be formed ultimately. Just as Fig. 1(c) and (d) shows, the interconnecting and microporous structure still regularly exists in PAA-g-CTAB/PANI hybrid polymer and no obvious morphology changes can be observed, which imply that the introduction of PANI into the superabsorbent will not affect the absorption properties.

3.2. Liquid absorbency and conductivity of PAA-g-CTAB and PAA-g-CTAB/PANI polymers

The liquid electrolyte absorbency capability and conductivity properties of PAA-g-CTAB (a) and PAA-g-CTAB/PANI (b) polymers were measured and listed in Table 1. From which we can see that the swelling ratio (SR, g/g) of PAA-g-CTAB and PAA-g-CTAB/PANI was measured as 18.53 and 17.69 (g/g) respectively, which is relatively higher than other polymer hosts [6,28]. Besides, the former PAA-g-CTAB can absorb a little more liquid electrolyte than PAA-g-CTAB/PANI, the small amount of decrease in liquid absorbency may arise from the introduction of PANI molecule inside of the polymer network, which results in a larger crosslinking density of the composite and leads to a decreased liquid absorbency [29].

Using the PAA-g-CTAB and PAA-g-CTAB/PANI superabsorbents as polymer host to prepare gel-electrolytes used in DSSCs, owing to the large amounts of liquid electrolyte absorbed in the

Table 1
Liquid absorbency (SR) and conductivity (σ) properties of the superabsorbent polymers.

Superabsorbents	SR (g/g)	σ (mS/cm) (20 °C)
PAA-g-CTAB (a)	18.53	11.35
PAA-g-CTAB/PANI (b)	17.69	14.29

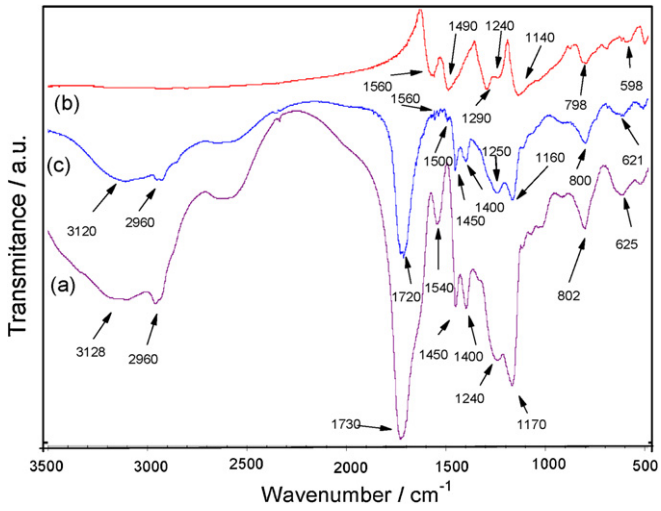

Fig. 2. FTIR spectra of PAA/CTAB (a), PANI (b), and PAA/CTAB/PANI (c).

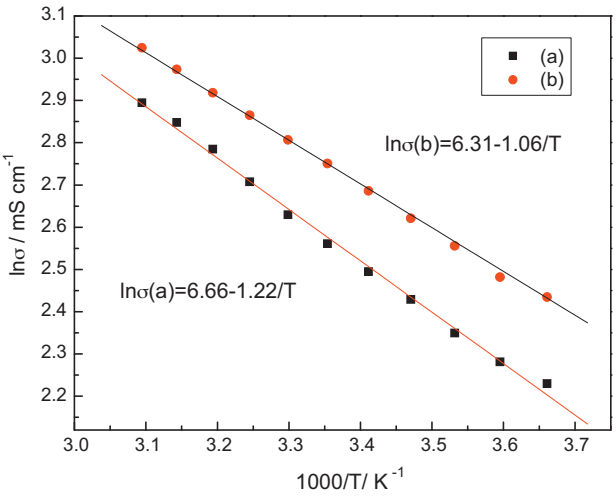

Fig. 3. Temperature dependence of the ionic conductivity (σ) for gel-electrolytes with PAA-g-CTAB (a) and PAA-g-CTAB/PANI (b) as polymer host.

gel-electrolyte, the ionic mobility and the connection between gel-electrolyte and TiO_2 film can be improved, which is benefited for the photovoltaic performance of DSSC. From Table 1, we can see that the conductivity (σ) of PAA-g-CTAB and PAA-g-CTAB/PANI were measured as 11.90 and 14.29 mS cm^{-1} (at 20 °C) respectively, and the best result is relatively higher than the previously published reports [6,28,30]. Though the liquid absorbency of PAA-g-CTAB is a little higher than PAA-g-CTAB/PANI, the conductivity of PAA-g-CTAB/PANI is higher than PAA-g-CTAB because of the introduction of the conductivity PANI polymer chains inside of the polymer. It can be confirmed that the DSSC based on PAA-g-CTAB/PANI hybrid superabsorbent can reach an improved photovoltaic performance.

3.3. FTIR spectra of samples

Fig. 2 shows the FTIR spectroscopy of PAA/CTAB (a), PANI (b), PAA/CTAB/PANI (c). Curve (a) for PAA/CTAB shows a middle strong and broad absorption band at 3300–3100 cm^{-1}, which can be attributed to O–H stretching modes, and the peaks at 1242 and 918 cm^{-1} are attributed to the O–H wagging vibration and bending vibration, respectively. The absorption peak at 2960 cm^{-1} is for –CH_3, and the band centers at 1450, 1400, 802, 625 cm^{-1} arise from the –CH_2-wagging vibration, –CH_3 scissoring vibrations, C–H out-of-plane bending vibration, C–H out-of-plane deformation vibration, respectively. The characteristic peaks at 1730 cm^{-1} are responsible for C=O bending in COOH and the peak at 1170 cm^{-1} is due to C–O–C stretching vibration [27,28,31,32].

For PANI in curve (b), the characteristic peaks of PANI present near the wavenumbers of 1560 cm^{-1} (C–C stretching mode for the quinoid ring), 1490 cm^{-1} (benzenoid rings vibration), 1290 cm^{-1} (aromatic C–N stretching mode), 1240 cm^{-1} (C–N^+ stretching vibration), 1140 cm^{-1} (C–H in-plane deformation), and 798 cm^{-1} (out-of-plane bending vibration of C–H), 598 cm^{-1} (out-of-plane deformation vibration of C–H), coincide with the previous reports [33–37].

For PAA-g-CTAB/PANI, curve (c) shows a similar FTIR spectrum as curve (a) except for some new peaks emerge in curve (c), such as the peaks at 1560, 1500 cm^{-1} responsible for C–C stretching mode for the quinoid ring and benzenoid in PANI. Besides, the C–H out-of-plane bending vibration (at 800 cm^{-1}), C–H out-of-plane deformation vibration (at 621 cm^{-1}) shows a little red shift. Additionally, the peak at 1720 arised from C = O bending in –COOH split into two peaks, which may be caused by the hydrogen bond interaction formed in the hybrid polymeric components after the introduction of PANI [14]. Summarily, the peak center changes indicate that the PANI is formed inside of PAA-g-CTAB polymer network.

3.4. Influence of temperature on the conductivity of gel-electrolyte

The conductivity–temperature (σ–T) relationships for the gel-electrolytes with PAA-g-CTAB (a) and PAA-g-CTAB/PANI (b) are shown in Fig. 3. From Fig. 3, we can see that the conductivity increased with the increase of temperature and the ln (σ) versus 1/T plots is almost linear, which coincides with our previous results [28,30,38]. The σ–T behavior for the gel-electrolytes based on PAA-g-CTAB (a) and PAA-g-CTAB/PANI (b) can be described by the Arrhenius equation (4) shown as follows:

$$\ln \sigma = \ln A - \frac{E_a}{RT} \quad (4)$$

where σ is the conductivity, E_a is the activation energy, R is the molar gas constant, A is a meaningless constant, and T is absolute temperature. According to the experimental data, the E_a and A for the gel-electrolyte based on PAA-g-CTAB/PANI are calculated as 8.84 kJ mol^{-1} and 780, and the E_a and A for the gel-electrolyte based on PAA-g-CTAB are calculated as 10.12 kJ mol^{-1}, 552, respectively. Clearly, the gel-electrolytes with (b) has lower E_a and A than that with PAA-g-CTAB, which indicates a faster transportation rate of I^-/I_3^- in PAA-g-CTAB/PANI hybrid. In one word, the introduction of PANI to the polymer system has a positive effect on ionic conductivity of gel-electrolyte. In general, when an ionic transport process involves intermolecular ion hopping, the conductivity is determined by the thermal hopping frequency, which in turn is proportional to exp($-E/kT$), and this leads to an Arrhenius conductivity–temperature relationship [6]. The ion hopping increases with an increase of temperature, which enhances the conductivity of the system.

3.5. Photovoltaic performance of DSSC

Under illumination with a simulated solar light of 100 mW cm^{-2} (AM 1.5), photocurrent–voltage curves of DSSCs based on gel-electrolytes with PAA-g-CTAB (a) and PAA-g-CTAB/PANI (b) were measured and shown in Fig. 4. The photoelectric parameters of DSSCs such as short circuit photocurrent density (J_{sc}), open circuit voltage (V_{oc}), fill factor (FF) and the overall energy conversion efficiency (η) are listed in Table 2. It is evident that all

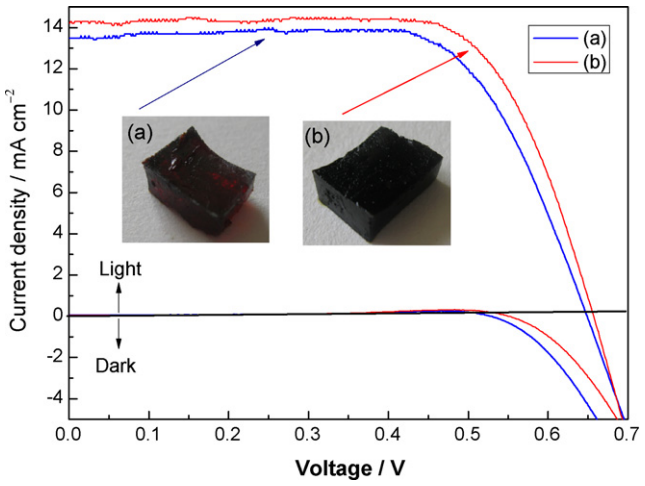

Fig. 4. Photocurrent–voltage curve of DSSC with gel-electrolytes based on PAA-g-CTAB (a) and PAA-g-CTAB/PANI (b) (inset: digital photos of (a) and (b)).

Table 2
Photovoltaic performance of DSSCs with PAA-g-CTAB (a) and PAA-g-CTAB/PANI (b).

Gel electrolyte	J_{sc} (mA cm^{-2})	V_{oc} (V)	FF	η (%)
PAA-g-CTAB (a)	13.5	0.649	0.703	6.15
PAA-g-CTAB/PANI (b)	14.2	0.657	0.715	6.68

photoelectric parameters of the DSSC with PAA-g-CTAB/PANI based gel-electrolyte are higher, which is higher than that of the DSSC with PAA-g-CTAB based gel-electrolyte.

The η of PAA-g-CTAB/PANI reaches 6.68%, while which of PAA-g-CTAB is only 6.15%. The increased light-to-electron efficiency of PAA-g-CTAB/PANI compared with that of PAA-g-CTAB attributes to the increased conductivity because of the introduction of PANI into the superabsorbent network. As measured above, the introduction of PANI molecule leads to a decreased E_a (from 10.12 to 8.84 kJ mol^{-1}) and a faster transportation rate of I^-/I_3^- in PAA-g-CTAB/PANI hybrid polymer; besides, as pointed in the previous work [29], PANI has a good electrocatalytic activity for the I_3^-/I^- redox reaction, which causes a lower energy lose from I_3^- to I^-, the above two reasons result in an increased J_{sc} (from 13.5 to 14.2 mA cm^{-2}) and an enhanced η. In one word, the addition of PANI into the gel-electrolyte is an efficient way to enhance the photovoltaic performance of DSSCs.

Additionally, the dark current of (b) is decreased than that of (a), which indicates a high utilization of I_3^- in the gel-electrolyte based on PAA-g-CTAB/PANI hybrid polymer. As we know, the dark current is attributed to the I_3^- reduction by conduction band electrons at the semiconductor electrolyte junction [Eq. (5)] [39], in order to suppress the dark current reaction, it should decrease the connection between I_3^- and TiO_2 film and accelerate the reduction of I_3^- on Pt counter electrode.

$$I_3^- + 2e_{cb}^-(TiO_2) = 3I^- \quad (5)$$

As can be seen from the SEMs in Fig. 1, large amounts of microporous holes still exist inside of PAA-g-CTAB/PANI hybrid polymer host, we can deduce that when aniline monomer is absorbed inside of the PAA-g-CTAB network, the polyaniline chain grows along the PAA-g-CTAB polymer chain during the second polymerization process [22]. Because of that the PAA-g-CTAB/PANI polymer host has an improved conductivity, the transportation rate of I^-/I_3^- is faster than that in PAA-g-CTAB polymer host, so the I_3^- can be more fastly transported to the Pt-coated counter electrode and more efficiently reduced at the counter electrode instead of recombination with TiO_2 anode film. In summary, the second growth of PANI inside of PAA-g-CTAB network leads to a suppressed dark current and a higher light-current.

The inset is the digital photos of gel-electrolyte based on PAA-g-CTAB and PAA-g-CTAB/PANI, from which we can see that the former is dark red while the later is completely black which aroused by the formation of PANI inside of the polymer. The color changes of gel-electrolytes of PAA-g-CTAB and PAA-g-CTAB/PANI vividly prove the synthesis of the modified PAA-g-CTAB/PANI hybrid superabsorbent.

4. Conclusions

A PAA-g-CTAB/PANI hybride modified superabsorbent was synthesized by a two-step solution polymerization. Using this polymer hybrid as host to fabricate gel-electrolyte, a gel-electrolyte with an ionic conductivity of 14.29 mS cm^{-1} (at 20 °C) was obtained. By sandwiching a slice of the obtained gel-electrolyte between a dye sensitized TiO_2 electrode and a platinum counter electrode, a cell with photocurrent density of 14.2 mA cm^{-2}, open circuit potential of 657 mV, fill factor of 0.715 and efficiency of 6.68% was fabricated. From the SEM observation of the synthesized polymer, large amounts of closed-microporous holes exist inside the polymer. The σ–T relationship and I–V test results show that the addition of PANI has a positive effect on the gel-electrolyte and the photovoltaic performance.

Acknowledgments

The authors thank for the joint support by the National High Technology Research and Development Program of China (No. 2009AA03Z217), the National Natural Science Foundation of China (Nos. 90922028, 50842027).

References

[1] B. O'Regan, M. Gratzel, Nature 353 (1991) 737.
[2] M. Gratzel, Nature 414 (2001) 338.
[3] M. Gratzel, Acc. Chem. Res. 42 (2009) 1788.
[4] Y. Cao, Y. Bai, Q. Yu, Y. Cheng, S. Liu, D. Shi, F. Gao, P. Wang, J. Phys. Chem. C 113 (2009) 6290.
[5] J. Wu, S. Hao, Z. Lan, J. Lin, M. Huang, Y. Huang, L. Fang, S. Yin, T. Sato, Adv. Funct. Mater. 17 (2007) 2645.
[6] J. Wu, Z. Lan, J. Lin, M. Huang, S. Hao, T. Sato, S. Yin, Adv. Mater. 19 (2007) 4006.
[7] E. Lancelle-Beltran, P. Prene, C. Boscher, P. Belleville, P. Buvat, C. Sanchez, Adv. Mater. 18 (2006) 2579.
[8] S. Tan, J. Zhai, M. Wan, Q. Meng, Y. Li, L. Jiang, D. Zhu, Phys. Chem. B 108 (2004) 18693.
[9] J. Wu, S. Hao, Z. Lan, J. Lin, M. Huang, Y. Huang, P. Li, S. Yin, T. Satot, J. Am. Chem. Soc. 130 (2008) 11568.
[10] M. Biancardo, R. Argazzi, C. Bignozzi, Inorg. Chem. 44 (2005) 9619.
[11] P. Wang, S. Zakeeruddin, P. Comte, I. Exnar, M. Gratzel, J. Am. Chem. Soc. 125 (2003) 1166.
[12] P. Wang, S. Zakeeruddin, J. Moser, M. Gratzel, J. Phys. Chem. B 107 (2003) 13280.
[13] P. Wang, S. Zakeeruddin, R. Humphry-Baker, M. Gratzel, Chem. Mater. 16 (2004) 2694.
[14] Z. Lan, J. Wu, S. Hao, J.M. Lin, M. Huang, Y. Huang, Energ. Environ. Sci. 2 (2009) 524.
[15] R. Komiya, L. Han, R. Yamanaka, A. Islam, T. Mitate, J. Photochem. Photobiol. A 164 (2004) 123.
[16] M. Biancardo, K. West, F. Krebs, Sol. Energy Mater. Sol. Cells 90 (2006) 2575.
[17] S. Lu, R. Koeppe, S. Gunes, N. Sariciftci, Sol. Energy Mater. Sol. Cells 91 (2007) 1081.
[18] M. Biancardo, K. West, F. Krebs, J. Photochem. Photobiol. A 187 (2007) 395.
[19] J. Wu, J. Lin, M. Zhou, Macromol. Rapid Commun. 21 (2000) 1032.
[20] J. Lin, J. Wu, Z. Yang, M. Pu, Macromol. Rapid Commun. 22 (2001) 422.
[21] W. Lee, Y. Chen, Eur. Polym. J. 41 (2005) 1605.
[22] Q. Tang, J. Lin, J. Wu, C. Zhang, S. Hao, Carbohydr. Polym. 67 (2007) 332.
[23] Q. Tang, J. Wu, H. Sun, J. Lin, S. Fan, D. Hu, Carbohydr. Polym. 74 (2008) 215.
[24] Q. Tang, J. Wu, J. Lin, S. Fan, D. Hu, J. Mater. Res. 24 (2009) 1653.
[25] J. Wu, Z. Lan, D. Wang, S. Hao, J. Lin, Y. Wei, S. Yin, T. Sato, J. Photochem. Photobiol. A 181 (2006) 333.
[26] J. Wu, P. Li, S. Hao, H. Yang, Z. Lan, Electrochim. Acta 52 (2007) 5334.
[27] T.K. Mudiyanselage, D.C. Neckers, Soft Matter 4 (2008) 768.
[28] Z. Tang, J. Wu, Q. Li, Z. Lan, L. Fan, J. Lin, M. Huang, Electrochim. Acta 55 (2010) 4883.

[29] Q. Li, J. Wu, Q. Tang, Z. Lan, P. Li, J. Lin, L. Fan, Electrochem. Commun. 10 (2008) 1299.
[30] Q. Li, J. Wu, Z. Tang, Y. Xiao, M. Huang, J. Lin, Electrochim. Acta 55 (2010) 2777.
[31] Z. Tang, X. Wu, Z. Luo, Q. Tang, J. Lin, J. Wu, Polym. Adv. Technol. (2011), on line.
[32] Q. Tang, J. Wu, Q. Li, J. Lin, Polymer 49 (2008) 5329.
[33] J. Tang, X. Jing, B. Wang, F. Wang, Synth. Met. 24 (1987) 231.
[34] R. David, M. Mohilner, J. William, Argersinger, J. Am. Chem. Soc. 84 (1962) 3618.
[35] A. Zimmermann, U. Künzelmann, L. Dunsch, Synth. Met. 93 (1998) 17.
[36] Y. Sahin, K. Pekmez, A. Yildiz, Synth. Met. 129 (2002) 107.
[37] Q. Qin, J. Tao, Y. Yang, Synth. Met. 160 (2010) 1167.
[38] Z. Lan, J. Wu, D. Wang, S. Hao, J. Lin, Y. Huang, Sol. Energy 80 (2006) 1483.
[39] J. He, G. Benko, F. Korodi, T. Polivka, R. Lomoth, B. Akermark, L. Sun, A. Hagfeldt, V. Sundstrom, J. Am. Chem. Soc. 124 (2002) 4922.